Available online at www.sciencedirect.com

ScienceDirect

IFAC PapersOnline CONFERENCE PAPER ARCHIVE

IFAC PapersOnLine 53-2 (2020) 15674–15679

Shortest Bounded-Curvature Paths Via Circumferential Envelope of a Circle

Bhargav Jha * **Zheng Chen** ** **Tal Shima** ***

* *Ph.D. Student, Department of Aerospace Engineering, Technion - Israel Institute of Technology, Haifa, Israel - 3200001 (e-mail: jhabhargav@campus.technion.ac.il).*
** *Researcher, School of Aeronautics and Astronautics, Zhejiang University, Hangzhou, China- 310027 (e-mail: z-chen@zju.edu.cn)*
*** *Professor, Department of Aerospace Engineering, Technion - Israel Institute of Technology, Haifa, Israel - 3200001 (e-mail: tal.shima@technion.ac.il)*

Abstract The paper characterizes the shortest bounded-curvature paths for a Dubins vehicle between two configurations with specified location and heading angle via the boundary of an intermediate circle. Only two distinct cases can arise in such engagements, first, when the shortest path is tangent to the circle at only one point, and second, when a segment of the shortest path overlaps a part of the circular boundary. Control command for both the cases are proposed, and some geometric properties for the first case are established by using necessary conditions for state inequality constraints and Pontryagin's maximum principle. Numerical examples are presented to illustrate the geometric properties of the shortest bounded-curvature paths. These geometric properties give insight about concatenation of different segments of the shortest path and allow us to state that the candidate shortest paths belong to a finite set.

Keywords: Dubins path, autonomous systems, path planning, motion control, optimal control

1. INTRODUCTION

In recent times, autonomous vehicles have become increasingly popular due to their wide applications such as surveillance, search and rescue, crop monitoring, and driver-less transportation. These vehicles operate in various environments such as land, air, marine, and in space. In most real world scenarios, motion planning of these vehicles from an initial point to the target point involves satisfying various constraints. Most of these constraints are vehicle-specific and the remainder arise from the complexity of the traversed environment. The vehicle specific constraints take into account the vehicle's dynamic and kinematic aspects such as the minimum speed, the maximum maneuver capabilities, and the response of the vehicle. Environment specific constraints include presence of obstacles or adverse regions where it is prohibited to enter.

A popular problem in motion planning aims at finding time optimal trajectories between two configurations in $SE(2)$ (location and heading orientation), for unidirectional vehicles with constant speed subjected to bounded-curvature constraints. This problem is an infinite dimensional optimisation problem and was first proposed by Markov (1887) in context of railway track design. Dubins (1957) has proposed that the solution for this problem belongs to a finite set of 6 types of trajectories using geometrical analysis. Such vehicles are popularly denoted as Dubins vehicle and the aforementioned problem is called Dubins two-point problem. With the advent of maximum principle by Pontryagin et al. (1961), an alternate proof was proposed in Johnson (1974) and Boissonnat et al. (1994). Extension of this problem for a bidirectional vehicle was solved by Reeds and Shepp (1990) and an alternate proof for this using geometric optimal control theory was proposed by Sussmann and Tang (1991).

With the increasing emergence of practical applications of such problems, various classes of problems have stemmed out from the Dubins two-point problem. For example, the Dubins travelling salesman problem (DTSP) aims at finding the shortest bounded-curvature path among a finite set of n configurations such that each point is visited exactly once. Ny et al. (2011) have proven that solution of such problems is NP-hard, thereby justifying the development of approximate and heuristic approaches to solve it. In the same paper as well as in Isaiah and Shima (2015), discretization based heuristic approaches have been proposed to solve DTSP. Recently, using maximum principle, Chen and Shima (2019) have considered DTSP with three points and provided a complete analytical solutions for all possible shortest bounded-curvature trajectories. They have also highlighted the superiority of the proposed approach over direct discretization based approaches. Another class of problems that finds wide practical applications are DTSP with neighbourhoods (DTSPN). They differ from DTSP in a way that the target points can have a region around them and each of these regions must be visited once. Heuristic and algorithmic based approaches have been proposed for these problems by Zhang et al. (2014), Isaacs and Hespanha (2013), Pěnička et al. (2017), and the references therein. The problem is also shown to be NP-hard. But there is a gap to fill for the analytical solution of the simplest case of DTSPN. Finding such analytical solutions will reduce the computational complexity and give more insights into the properties of optimal trajectories.

10.1016/j.ifacol.2020.12.2554

In this paper, we consider a DTSPN-like problem where we find time-optimal path of a Dubins vehicle from an initial configuration to a final configuration via an intermediate circle. The objective here is to necessarily reach the boundary of the circle but avoid entering inside the circular region at all times. Some of the key applications for this research covers surveillance and imaging of restricted regions by a fixed-wing unmanned aerial vehicle (UAV), and avoiding obstacles which interfere with the shortest path between two configurations.

2. PROBLEM FORMULATION

Consider a circular region of radius $r \in \mathbb{R}^+$ with its center at the origin of an inertial coordinate system. For notational simplicity, we denote this circle by $\mathscr{C}$, *i.e.*,

$$\mathscr{C} = \{(x, y) \in \mathbb{R}^2 | x^2 + y^2 = r^2\}$$

In this coordinate system, the state $\mathbf{x} = [x, y, \theta]^T$, also called configuration, represents the position $(x, y) \in \mathbb{R}^2$ and the orientation $\theta \in \mathbb{S}^1$ of a Dubins vehicle with minimum turn radius $\rho \in \mathbb{R}^+$. The kinematics of this vehicle evolves according to the following system of differential equations.

$$\frac{\mathrm{d}\mathbf{x}}{\mathrm{d}t} = f(\mathbf{x}, u), \qquad u \in [-1, 1] \tag{1}$$

where $f(x, u)$ is given as,

$$f(\mathbf{x}, u) = \begin{bmatrix} \cos\theta \\ \sin\theta \\ \dfrac{u}{\rho} \end{bmatrix} \tag{2}$$

Here, u is the control input and t denotes time.

The problem here is to find the shortest path for Dubins vehicle from an initial configuration $\mathbf{x_0} = (x_0,\ y_0,\ \theta_0)$ at time t_0 to a given final configuration $\mathbf{x_f} = (x_f,\ y_f,\ \theta_f)$ via the circle $\mathscr{C}$. The engagement geometry is shown in Fig. 1. We denote the time at which the Dubins vehicle reaches the final configuration as t_f, the time at which it reaches the circle $\mathscr{C}$ as $t_1 \in (t_0, t_f)$, and the time when it leaves the circle $\mathscr{C}$ as $t_2 \in [t_1, t_f)$.

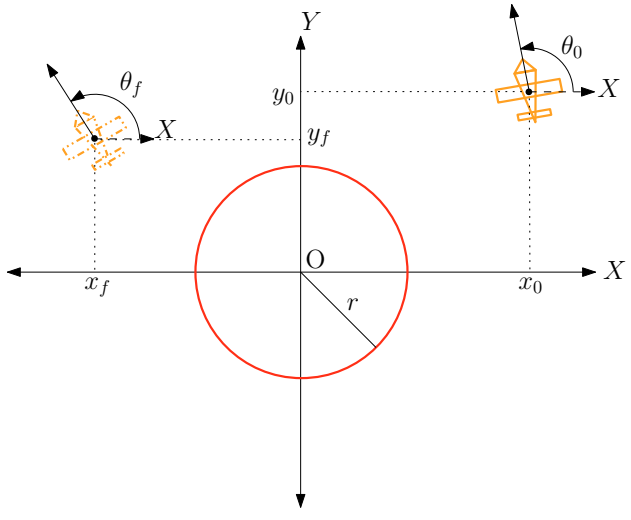

Figure 1. Engagement Geometry

To avoid entering inside the circle $\mathscr{C}$, the following state inequality constraint must be satisfied,

$$S(\mathbf{x}, t) = \frac{1}{2}\left(x^2 + y^2 - r^2\right) \geq 0 \tag{3}$$

At the final time, the following terminal constraint must also be satisfied.

$$\mathbf{M}(t_f) \triangleq \begin{bmatrix} x(t_f) - x_f & y(t_f) - y_f & \theta(t_f) - \theta_f \end{bmatrix}^T = [\mathbf{0}]_{3\times 1} \tag{4}$$

In order to find the shortest path, the cost function to be minimized is,

$$J = \int_{t_0}^{t_f} 1 \, \mathrm{d}t \tag{5}$$

3. OPTIMAL PATH GENERATION

The formulated problem is considered under the class of optimal control problems with terminal and state inequality constraints. Hartl et al. (1995) provides a concise review of the approaches to solve such problems. Here, we use the first order necessary conditions obtained by Bryson et al. (1963).

During the time interval when the path of the Dubins vehicle is on the circle $\mathscr{C}$, we have

$$S(\mathbf{x}, t) = 0 \qquad t \in [t_1, t_2]. \tag{6}$$

In this interval, the higher order derivatives of $S(\mathbf{x}, t)$ must also identically vanish. In order to make the constraint an explicit function of control u, we obtain the higher derivatives until u reappears.

$$S^{(1)} \triangleq \frac{\mathrm{d}S}{\mathrm{d}t} = x\cos\theta + y\sin\theta = 0 \tag{7}$$

$$S^{(2)} \triangleq \frac{\mathrm{d}^2 S}{\mathrm{d}t^2} = 1 + \left(y\cos\theta - x\sin\theta\right)\frac{u}{\rho} = 0 \tag{8}$$

From Eq. (8), $S^{(2)} = 0$ gives the control on the circular boundary as

$$u = -\frac{\rho}{\left(y\cos\theta - x\sin\theta\right)} \tag{9}$$

Remark 1. On the constraint boundary ($S = 0,\ S^{(1)} = 0$), the heading direction of the Dubins vehicle is tangent to the circle. Therefore, we have $\left|\left(y\cos\theta - x\sin\theta\right)\right| = r$ on the constraint boundary, where $|\cdot|$ denotes the absolute value. It should be noted that the control in Eq. (9) is only realizable if $r \geq \rho$.

In addition to the above conditions on the constrained boundary, the following conditions must also hold at the time of entering the constraint boundary (t_1) from the unconstrained path,

$$N(\mathbf{x_1}, t_1) \triangleq \begin{bmatrix} \dfrac{1}{2}[x(t_1)^2 + y(t_1)^2 - r^2] \\ x(t_1)\cos\theta(t_1) + y(t_1)\sin\theta(t_1) \end{bmatrix} = 0 \tag{10}$$

Remark 2. From Eq. (10), it is known that the heading direction of the Dubins vehicle will be tangent to the circumference of the circle at the point when it reaches the circle.

Let the costate vector be $\mathbf{p} = [p_x\ p_y\ p_\theta]^T$. According to Bryson et al. (1963), the Hamiltonian $H(\mathbf{p}, \mathbf{x}, u)$ of the problem can be written as,

$$\begin{aligned} H(\mathbf{p}, \mathbf{x}, u) &= p_0 + p_x\cos\theta + p_y\sin\theta + p_\theta\frac{u}{\rho} + \lambda(t)S^{(2)} \\ &= p_0 + p_x\cos\theta + p_y\sin\theta + \lambda(t) \\ &\quad + \frac{u}{\rho}\left(p_\theta + \lambda(t)\left(y\cos\theta - x\sin\theta\right)\right) \end{aligned} \tag{11}$$

where λ is a scalar given by

$$\lambda(t) = \begin{cases} >0, & \text{if } S(x,t)=0, \\ <0, & \text{if } S(x,t)>0 \end{cases} \tag{12}$$

Using variational approach, Bryson et al. (1963) have proposed the following first order necessary conditions,

$$\mathbf{p}(t_1^-) = \mathbf{p}(t_1^+) + \frac{\partial N(\mathbf{x},t)}{\partial x}^\top \boldsymbol{\mu}\Big|_{t=t_1} \tag{13a}$$

$$H(\mathbf{p}^*,\mathbf{x}^*,u^*)\big|_{t_1^-} = H(\mathbf{p}^*,\mathbf{x}^*,u^*)\big|_{t_1^+} \tag{13b}$$

$$\mathbf{p}(t_2^-) = \mathbf{p}(t_2^+) \tag{13c}$$

$$H(\mathbf{p}^*,\mathbf{x}^*,u^*)\big|_{t_2^-} = H(\mathbf{p}^*,\mathbf{x}^*,u^*)\big|_{t_2^+} \tag{13d}$$

Here, $\boldsymbol{\mu} = [\mu_1\ \mu_2]^T$ is a two-dimensional vector. This translates to following,

$$p_x(t_1^-) = p_x(t_1^+) + \mu_1 x(t_1) + \mu_2 \cos\theta(t_1) \tag{14a}$$

$$p_y(t_1^-) = p_y(t_1^+) + \mu_1 y(t_1) + \mu_2 \sin\theta(t_1) \tag{14b}$$

$$p_\theta(t_1^-) = p_\theta(t_1^+) + \mu_2\left(y(t_1)\cos\theta(t_1) - x(t_1)\sin\theta(t_1)\right) \tag{14c}$$

$$p_x(t_2^-) = p_x(t_2^+) \tag{14d}$$

$$p_y(t_2^-) = p_y(t_2^+) \tag{14e}$$

$$p_\theta(t_2^-) = p_\theta(t_2^+) \tag{14f}$$

Remark 3. In a special case when the optimal path is tangent to the intermediate circular boundary at only one point, only the conditions in Eq. (13b) and Eqs. (14a)-(14c) should be considered. In this case, these conditions are analogous to one interior point constraint.

Using transversality conditions to satisfy the terminal states we have,

$$\mathbf{p}(t_f) = \boldsymbol{\beta}^T \frac{\partial \mathbf{M}}{\partial \mathbf{x_f}} \tag{15}$$

where, $\boldsymbol{\beta} \in \mathbb{R}^3$ is a constant vector.

The costates should satisfy the following Euler-Lagrange equations,

$$\dot{\mathbf{p}} = \begin{cases} -\left[\dfrac{\partial f}{\partial \mathbf{x}}\right]^T \mathbf{p}, & S<0 \\ -\left[\dfrac{\partial f}{\partial \mathbf{x}} - \dfrac{\partial f}{\partial u}\left(\dfrac{\partial S^{(2)}}{\partial u}\right)^{-1}\dfrac{\partial S^{(2)}}{\partial \mathbf{x}}\right]^T \mathbf{p}, & S=0 \end{cases} \tag{16}$$

This gives us the following equations,

$$\dot{p}_x = \begin{cases} 0, & S>0 \\ \dfrac{-p_\theta \sin\theta}{x\sin\theta - y\cos\theta}, & S=0 \end{cases} \tag{17a}$$

$$\dot{p}_y = \begin{cases} 0, & S>0 \\ \dfrac{p_\theta \cos\theta}{x\sin\theta - y\cos\theta}, & S=0 \end{cases} \tag{17b}$$

$$\dot{p}_\theta = \begin{cases} p_x\sin\theta - p_y\cos\theta, & S>0 \\ \dfrac{-p_x(t)\sin\theta + p_y(t)\cos\theta}{r^2}, & S=0 \end{cases} \tag{17c}$$

We denote by t_i^- and t_i^+ the time just before and after t_i (i=1,2), respectively. From Eqs. (17) we obtain the expression for p_θ as,

$$p_\theta(t) = \begin{cases} p_x(t_1^-)y - p_y(t_1^-)x + c_1, & t\in[t_0,t_1^-) \\ p_x(t_2^+)y - p_y(t_2^+)x + c_2, & t\in(t_2^+,t_f] \end{cases} \tag{18}$$

In addition to it, eliminating μ_1 and μ_2 from Eqs. (14a)-(14c) we have the following expression,

$$p_x(t_1^-)y(t_1) - p_y(t_1^-)x(t_1) = p_x(t_1^+)y(t_1) - p_y(t_1^+)x(t_1) + \mu_2(y(t_1)\cos\theta(t_1) - x(t_1)\sin\theta(t_1)) \tag{19}$$

Combining this equation with Eq. (18) leads to

$$p_\theta(t_1^+) = c_1 + p_x(t_1^+)y(t_1) - p_y(t_1^+)x(t_1) \tag{20}$$

Now, using maximum principle by Pontryagin et al. (1961) to obtain the optimal control (u^*) at unconstrained path ($S \geq 0$) we get,

$$u^* = \underset{u\in[-1,1]}{\arg\max}\, H(\mathbf{p},\mathbf{x},u) \implies u^* = \begin{cases} -1 & p_\theta < 0 \\ 0 & p_\theta = 0 \\ 1 & p_\theta > 0 \end{cases} \tag{21}$$

On the constrained arc, the control will given by Eq. (9). This shows that the time optimal path can only be a concatenation of three categories of segments namely, straight line (S), circular arc (C) with radius ρ which can either be a right (R) turn or a left turn (L), and circular arc (O) with radius r. Also, the O segment can appear only at the boundary of the circle $\mathscr{C}$.

4. CHARACTERIZING THE OPTIMAL PATH

There are only two distinct cases for the tangency between the optimal path and the intermediate circle $\mathscr{C}$: (1) the optimal path has only one point tangent to $\mathscr{C}$ and (2) the optimal path overlaps the circle $\mathscr{C}$ on a nonzero interval. In this section, we will characterize the properties of time optimal paths for the first case. Geometric property for the second case are suggested later in Section 5.2 based on the results observed from numerical simulations.

In subsequent proofs, for notational simplicity we denote control input just before and after the tangent point as u^- and u^+, respectively.

Lemma 1. If there is only one point tangent at time t_1 to the intermediate circle $\mathscr{C}$ and if $u^- = u^+$, then $p_\theta\left(t_1^-\right) = p_\theta\left(t_1^+\right)$.

Proof. Let us denote $u^- = u^+ = u^1$. From Remark 3 and necessary condition in Eq. (13b), we have,

$$H(\mathbf{p}^*,\mathbf{x}^*,u^*)\big|_{t_1^-} = H(\mathbf{p}^*,\mathbf{x}^*,u^*)\big|_{t_1^+} \tag{22}$$

This condition gives rise to,

$$p_0 + p_x\left(t_1^-\right)\cos\theta\left(t_1^-\right) + p_y\left(t_1^-\right)\sin\theta\left(t_1^-\right) + p_\theta\left(t_1^-\right)\frac{u^-}{\rho} = p_0 + p_x\left(t_1^+\right)\cos\theta\left(t_1^+\right) + p_y\left(t_1^+\right)\sin\theta\left(t_1^+\right) + p_\theta\left(t_1^+\right)\frac{u^+}{\rho} \tag{23}$$

Using the necessary conditions (14a)-(14c) along with the fact that the states $\left(x,y,\theta\right)$ are continuous at t_1, we can rewrite Eq. (23) as,

$$\mu_1 x(t_1)\cos\theta(t_1) + \mu_2\cos^2\theta(t_1) + \mu_1 y(t_1)\sin\theta(t_1) + \mu_2\sin^2\theta(t_1) + \mu_2 y(t_1)\cos\theta(t_1)\frac{u^1}{\rho} - \mu_2 x(t_1)\sin\theta(t_1)\frac{u^1}{\rho} = 0 \tag{24}$$

Using the tangency condition $S^{(1)} = 0$ we have,

$$\mu_2 + \mu_2\left(y(t_1)\cos\theta(t_1) - x(t_1)\sin\theta(t_1)\right)\frac{u_1}{\rho} = 0$$

$$\implies u_1 = -\frac{\rho}{\left(y(t_1)\cos\theta(t_1) - x(t_1)\sin\theta(t_1)\right)} \text{ or } \mu_2 = 0 \tag{25}$$

From the expression of control on the constraint path in Eq.(9) and the first part of Eq. (25), it can be inferred that this control will drive the vehicle to move along the circle $\mathscr{C}$. This will contradict the fact that there is only one tangent point.

Hence $\mu_2 = 0$ and thus from Eq. (14c), we have $p_\theta\left(t_1^-\right) = p_\theta\left(t_1^+\right)$, completing the proof. □

Lemma 2. The segment of the optimal path before the tangent point is a straight line if and only if the segment after the tangent point is a straight line.

Proof. Rearranging Eq. (23) and using the necessary conditions from Eqs. (14a)-(14c) give us the following two equivalent form,

$$\rho\mu_2 + \mu_2\left(y(t_1)\cos\theta(t_1) - x(t_1)\sin\theta(t_1)\right)u^- + \left(u^- - u^+\right)p_\theta\left(t_1^+\right) = 0 \tag{26a}$$

$$\rho\mu_2 + \mu_2\left(y(t_1)\cos\theta(t_1) - x(t_1)\sin\theta(t_1)\right)u^+ + \left(u^- - u^+\right)p_\theta\left(t_1^-\right) = 0 \tag{26b}$$

Let us first consider the *necessary* condition that if the segment before t_1 is a straight line, implying $u^+ = 0$, which further implies $p_\theta\left(t_1^+\right) = 0$. Therefore from Eq. (26a) we obtain,

$$\mu_2\left(\rho + \left(y(t_1)\cos\theta(t_1) - x(t_1)\sin\theta(t_1)\right)u^-\right) = 0 \tag{27}$$

Using similar arguments as used in end of the proof for Lemma 1, we know that $\mu_2 = 0$ implying $p_\theta\left(t_1^-\right) = p_\theta\left(t_1^+\right) = 0$. Therefore, the segment after t_1 is a straight line if that before t_1 is a straight line.

Using Eq. (26b), the *sufficieny* condition can be completed along the same lines as above, thus completing the proof. □

Lemma 3. Given $\rho > r$, if the segment of the optimal path before t_1 is C^- and the segment after is C^+, then C^- and C^+ must have the same turning direction.

Proof. This will be proven by contradiction. Assume that both C^- and C^+ have different turning directions. For the sake of brevity let us define, $\gamma \triangleq \left(y(t_1)\cos\theta(t_1) - x(t_1)\sin\theta(t_1)\right)$. From Remark 1, we know that $|\gamma| = r$. From Eq. (26), we rewrite the following two equivalent forms of Eq. (23) as,

$$\mu_2\rho + \mu_2\gamma u^+ + p_\theta\left(t_1^-\right)\Delta u = 0 \tag{28a}$$

$$\mu_2\rho + \mu_2\gamma u^- + p_\theta\left(t_1^+\right)\Delta u = 0 \tag{28b}$$

where $\Delta u \triangleq u^- - u^+$. This gives us the following two equations which must also be equivalent,

$$p_\theta\left(t_1^-\right) = -\mu_2\frac{\left(\rho + \gamma u^+\right)}{\Delta u} \tag{29a}$$

$$p_\theta\left(t_1^+\right) = -\mu_2\frac{\left(\rho + \gamma u^-\right)}{\Delta u} \tag{29b}$$

From Lemma 2 and the contradictory assumption that the turn directions are opposite, there are only following two possible cases,

1. $u^- = -1$ implying $u^+ = +1$, $p_\theta\left(t_1^-\right) < 0$, $p_\theta\left(t_1^+\right) > 0$, and $\Delta u = -2$
2. $u^- = +1$ implying $u^+ = -1$, $p_\theta\left(t_1^-\right) > 0$, $p_\theta\left(t_1^+\right) < 0$, and $\Delta u = 2$.

Let us consider the first case. The idea behind the proof is that if we substitute the variables u^-, Δu, p_θ^- and p_θ^+ in both parts of Eq. (29), then given that $\rho > r$, there must be a consistent value of μ_2 that satisfies both the parts of the Eq. (29). Without loss of generality, let us assume $\gamma = r$. For $\gamma = -r$, the arguments below will still hold. Hence, we have from the first part of Eq. (29),

$$\left(p_\theta\left(t_1^-\right) = -\mu_2\frac{\left(\rho + r\right)}{\Delta u}\right) < 0 \tag{30}$$

As $\Delta u < 0$ and $\rho + r > 0$, this implies $\mu_2 < 0$. And from the second part of Eq. (29), we have,

$$\left(p_\theta\left(t_1^+\right) = -\mu_2\frac{\left(\rho - r\right)}{\Delta u}\right) > 0 \tag{31}$$

As $\Delta u < 0$ and $\rho - r > 0$, this implies $\mu_2 > 0$. So from Eqs. (30) and (31), we know that μ_2 can not have a consistent value, if we assume $\rho > r$ and the turn directions are opposite. This is a contradiction.

The proof for the second case is along the same lines and we arrive at the same contradiction. Therefore, the turn directions must be same, thereby completing the proof. □

Lemma 4. Given $\rho < r$, if the segment of the optimal path before t_1 is C^- and the segment after is C^+, then C^- and C^+ should have same turning direction.

Proof. As the path to the constrained boundary must be tangent to the circle, therefore C^- should be tangent to the circle at time t_1. If C^+ is of opposite turn direction than C^-, then as $r > \rho$, the path will enter inside circle $\mathscr{C}$ violating Eq. (3). □

Corollary 1. The segment of the path before and after the tangent point can only be one of the types from the set $\{R|R,\ L|L,\ S|S\}$, where '|' represent the concatenation of the segments.

Proof. The proof follows immediately from Lemmas 2-4. □

It should be noted that the solutions both before and after t_1 is of type CSC or CCC or their substrings due to Dubins (1957). Therefore, by Bellman's optimality principle (Bellman (1966), the optimal path can belong to either of the 36 types CSC|CSC, CSC|CCC, CCC|CSC, and CCC|CCC. But using Corollary 1, the optimal path candidates can be reduced to one of the 18 types such as CSCSC, CSCCC, CCCSC, and CCCCC or their substring.

Theorem 4.1. Let $\mathscr{L}_1$ and $\mathscr{L}_2$ denote the line segments joining all the points with $p_\theta = 0$ before and after the tangent point, respectively. Then the point of tangency, the point of intersection of the two lines and the origin will be co-linear.

Proof. According to Eq. (18) and (20), we have $c_1 = c_2$. Then, the expression of p_θ is given by

$$p_\theta(t) = \begin{cases} p_x(t_1^-)y(t) - p_y(t_1^-)x(t) + c_1, & t \in [t_0, t_1) \\ p_x(t_1^+)y(t) - p_y(t_1^+)x(t) + c_1, & t \in (t_1, t_f] \end{cases} \tag{32}$$

The equations of line $\mathscr{L}_1$ and $\mathscr{L}_2$ will be given by $p_x(t_1^-)y(t) - p_y(t_1^-)x(t) + c_1 = 0$ and $p_x(t_1^+)y(t) - p_y(t_1^+)x(t) + c_1 = 0$. Solving these two equations simultaneously gives us the point of intersection (say (x_c, y_c)) as,

$$x_c = c_1\frac{p_x(t_1^-) - p_x(t_1^+)}{p_y(t_1^+)p_x(t_1^-) - p_x(t_1^+)p_y(t_1^-)}$$

$$y_c = c_1\frac{p_y(t_1^-) - p_y(t_1^+)}{p_y(t_1^+)p_x(t_1^-) - p_x(t_1^+)p_y(t_1^-)} \tag{33}$$

Using the necessary conditions from Eqs. (14a)-(14b) and the fact that $\mu_2 = 0$ from Corollary 1 and Lemma 1, we have the following relation,

$$\frac{x_c}{y_c} = \frac{x_1}{y_1} \tag{34}$$

This shows that points (x_1, y_1), (x_c, y_c), $(0,0)$ are colinear, thereby completing the proof. □

Corollary 2. Assume that the optimal path before t_1 is of type $C_1S_2C_3$ and that the path after t_1 is of type $C_4S_5C_6$, then the arc lengths of C_3 and C_4 from the tangent point are equal to each other.

Proof. From Eqs. (21) and (32), we have that $p_x(t_1^-)\,y - p_y(t_1^-)\,x + c_1 = 0$ and $p_x(t_1^+)\,y - p_y(t_1^+)\,x + c_1 = 0$ along S_2 and S_5, respectively. The perpendicular distances from the center of C_3 and C_4 to the two straight lines $p_x(t_1^-)\,y - p_y(t_1^-)\,x + c_1 = 0$ and $p_x(t_1^+)\,y - p_y(t_1^+)\,x + c_1 = 0$ are equal to each other, because S_2 and S_5 are tangent to C_3 and C_4, respectively. Then, using results from Theorem 4.1 it can be geometrically shown that the perpendicular distances from the tangent point $(x(t_1), y(t_1))$ to the two straight lines $p_x(t_1^-)\,y - p_y(t_1^-)\,x + c_1 = 0$ and $p_x(t_1^+)\,y - p_y(t_1^+)\,x + c_1 = 0$ are equal to each other. Therefore, we have that the lengths of C_3 and C_4 are identical, completing the proof. □.

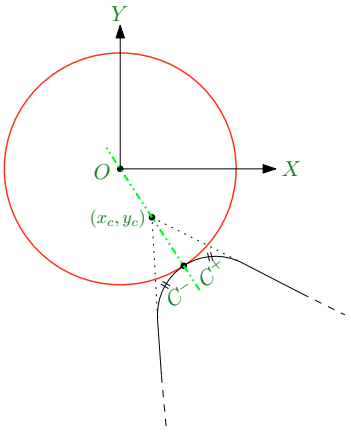

Figure 2. Geometrical properties for one tangent point case

Fig. 2 summarizes the properties of the optimal path shown by Theorem 4.1 and Corollary 2.

5. NUMERICAL SIMULATIONS

In this section, we present some numerical results showing the properties of the optimal path. We have used Falcon (Rieck et al., 2016) non-linear optimization tool to obtain the optimal paths. Two cases were simulated, first when the optimal path is tangent to the circular boundary and second when it overlaps the circular boundary. In both cases, the circle $\mathscr{C}$ with center at $(0,0)$ and radius $r = 4$ is considered.

5.1 Simulations: Optimal path with one point tangent to $\mathscr{C}$

In figure 3, the initial and final conditions are $\mathbf{x_0} = \left[-10, -15, -\frac{\pi}{4}\right]$ and $\mathbf{x_f} = [10, -15, \pi]$, respectively and $r > (\rho = 2)$. With the same initial and final configurations figure 4 shows the case with $r < (\rho = 6)$. In both these case, the results from Theorem 4.1 and Corolarry 2 can be verified. We can see that the arc lengths of the C-segment before and after the tangent point $(0, -4)$ are equal and the turn directions of the both the C-segments are same.

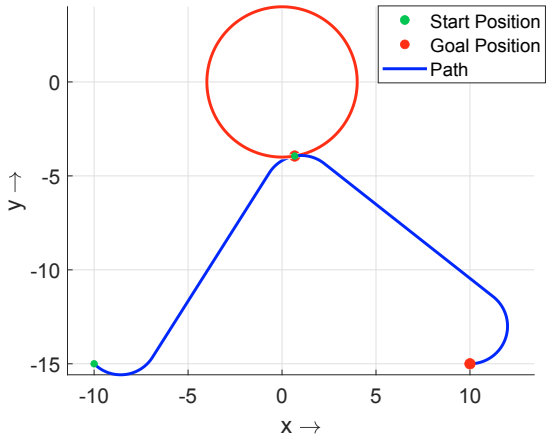

Figure 3. Optimal path with only one tangent point ($\rho < r$)

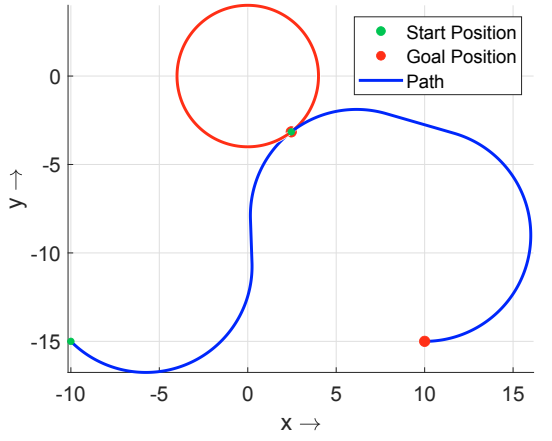

Figure 4. Optimal path with only one tangent point ($\rho > r$)

5.2 Simulations: Optimal path with an O-segment

In figure 5, the initial and final conditions are $\mathbf{x_0} = [-8, -8, -\pi]$ and $\mathbf{x_f} = \left[6, 8, \frac{3\pi}{4}\right]$, respectively. This figure as well as additional numerical simulations for different initial and final configurations suggest that an O-segment can be preceded and succeeded only by a S-segment. Theoretical proof for this property will be considered in future work.

6. CONCLUSIONS

The properties of the shortest bounded-curvature path between two configurations via an intermediate circle were derived using maximum principle and necessary conditions for state inequality constraints. It was shown that the optimal paths can consist of only C-segment, S-segment or O-segment. Finding these properties gives us insights about how these segments are concatenated and thereby leads to reduction in the number of candidate solutions from an infinite number of possible paths to a finite set. In the case where there is only one tangent point to the intermediate circle, the turn direction and arc length of the C segments prior and subsequent to the tangent point are equal. In addition to it, for optimal path of type CSCSC, the intersection point of two line segments, the center of the circle and the tangent point are colinear. Numerical examples justifying the

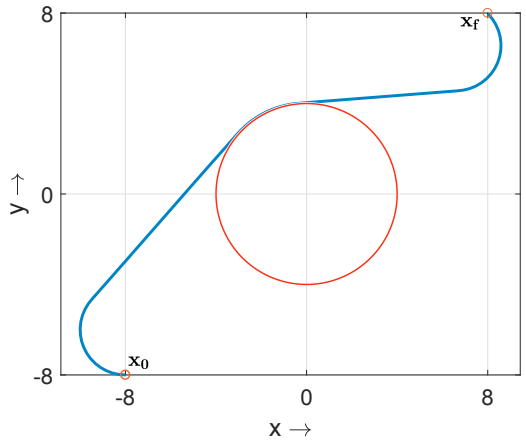

Figure 5. Optimal path with O-segment

established geometric properties were presented. Additionally, numerical simulations also suggested that for the case when a segment of the optimal path overlaps the circular boundary, an O-segment can be preceded and succeeded only by a S-segment. The proof of this property and analytical solutions for all possible candidate trajectories will be considered in our future work. Work in this direction is currently in progress.

ACKNOWLEDGEMENTS

This research was partially supported by the A. Pazy Research Foundation and National Natural Science Foundation of China under grant no. 61903331.

REFERENCES

Bellman, R. (1966). Dynamic programming. *Science*, 153(3731), 34–37.

Boissonnat, J.D., Cérézo, A., and Leblond, J. (1994). Shortest paths of bounded curvature in the plane. *Journal of Intelligent and Robotic Systems*, 11(1-2), 5–20.

Bryson, A.E., Denham, W.F., and Dreyfus, S.E. (1963). Optimal programming problems with inequality constraints. *AIAA journal*, 1(11), 2544–2550.

Chen, Z. and Shima, T. (2019). Shortest dubins paths through three points. *Automatica*, 105, 368–375.

Dubins, L.E. (1957). On curves of minimal length with a constraint on average curvature, and with prescribed initial and terminal positions and tangents. *American Journal of mathematics*, 79(3), 497–516.

Hartl, R.F., Sethi, S.P., and Vickson, R.G. (1995). A survey of the maximum principles for optimal control problems with state constraints. *SIAM review*, 37(2), 181–218.

Isaacs, J. and Hespanha, J. (2013). Dubins traveling salesman problem with neighborhoods: A graph-based approach. *Algorithms*, 6(1), 84–99.

Isaiah, P. and Shima, T. (2015). Motion planning algorithms for the dubins travelling salesperson problem. *Automatica*, 53, 247–255.

Johnson, H.H. (1974). An application of the maximum principle to the geometry of plane curves. *Proceedings of the American Mathematical Society*, 44(2), 432–435.

Markov, A.A. (1887). Some examples of the solution of a special kind of problem on greatest and least quantities. *Soobshch. Karkovsk. Mat. Obshch*, 1, 250–276.

Ny, J., Feron, E., and Frazzoli, E. (2011). On the dubins traveling salesman problem. *IEEE Transactions on Automatic Control*, 57(1), 265–270.

Pěnička, R., Faigl, J., Váňa, P., and Saska, M. (2017). Dubins orienteering problem with neighborhoods. In *2017 International Conference on Unmanned Aircraft Systems (ICUAS)*, 1555–1562. IEEE.

Pontryagin, L., Boltyanskii, V., Gamkrelidze, R., and Mishchenko, E. (1961). Mathematical theory of optimal processes {in Russian}.

Reeds, J. and Shepp, L. (1990). Optimal paths for a car that goes both forwards and backwards. *Pacific journal of mathematics*, 145(2), 367–393.

Rieck, M., Bittner, M., Grüter, B., and Diepolder, J. (2016). Falcon. m user guide. *Institute of Flight System Dynamics, Technische Universität München*.

Sussmann, H.J. and Tang, G. (1991). Shortest paths for the reeds-shepp car: a worked out example of the use of geometric techniques in nonlinear optimal control. *Rutgers Center for Systems and Control Technical Report*, 10, 1–71.

Zhang, X., Chen, J., Xin, B., and Peng, Z. (2014). A memetic algorithm for path planning of curvature-constrained uavs performing surveillance of multiple ground targets. *Chinese Journal of Aeronautics*, 27(3), 622–633.